ISPRS Journal of Photogrammetry and Remote Sensing 79 (2013) 80–93

Contents lists available at SciVerse ScienceDirect

ISPRS Journal of Photogrammetry and Remote Sensing

journal homepage: www.elsevier.com/locate/isprsjprs

Semi-automated extraction and delineation of 3D roads of street scene from mobile laser scanning point clouds

Bisheng Yang [a,*], Lina Fang [a], Jonathan Li [b]

[a] State Key Laboratory of Information Engineering in Surveying, Mapping and Remote Sensing, Wuhan University, Wuhan 430079, China
[b] Department of Geography & Environmental Management, University of Waterloo, Waterloo, Ontario, Canada N2L 3G1

ARTICLE INFO

Article history:
Received 19 August 2012
Received in revised form 21 January 2013
Accepted 29 January 2013

Keywords:
Mobile laser scanning
Curb detection
3D road extraction
Scanning lines
Moving windows filtering

ABSTRACT

Accurate 3D road information is important for applications such as road maintenance and virtual 3D modeling. Mobile laser scanning (MLS) is an efficient technique for capturing dense point clouds that can be used to construct detailed road models for large areas. This paper presents a method for extracting and delineating roads from large-scale MLS point clouds. The proposed method partitions MLS point clouds into a set of consecutive "scanning lines", which each consists of a road cross section. A moving window operator is used to filter out non-ground points line by line, and curb points are detected based on curb patterns. The detected curb points are tracked and refined so that they are both globally consistent and locally similar. To evaluate the validity of the proposed method, experiments were conducted using two types of street-scene point clouds captured by Optech's Lynx Mobile Mapper System. The completeness, correctness, and quality of the extracted roads are over 94.42%, 91.13%, and 91.3%, respectively, which proves the proposed method is a promising solution for extracting 3D roads from MLS point clouds.

1. Introduction

Semi-automated and automated road extraction from various geo-spatial data sources has attracted a large amount of attention in the fields of photogrammetry, remote sensing, and computer vision. The extraction of roads from remote sensing images has been studied using various methods, such as edge detection or texture analysis (Ferchichi and Wang, 2005; Wan et al., 2007), geometric deformable modeling (Laptev et al., 2000; Niu, 2006; Peng et al., 2008), machine learning (Zhang et al., 2001; Barsi and Heipke, 2003), and stochastic geometry modeling (Brazohar and Cooper, 1996; Lacoste et al., 2005, 2010; Lafarge et al., 2010). These methods achieve their best road extraction results in rural environments, where color or intensity is relatively distinctive and consistent within road areas. However, automated road extraction from high resolution images in dense urban environments is difficult because of building shadows, trees, and moving objects, which lead to unreliable and incomplete road extraction (Hu et al., 2004).

Recent advances in laser scanning technology have lead to the integration of laser scanners, navigation sensors (typically included Global Navigation Satellite Systems and Inertial Measurement Unit), and other data acquisition sensors (e.g., digital cameras) with mobile mapping platforms (Barber et al., 2008). Mobile laser scanning (MLS) has become a cost-effective solution for capturing very dense point clouds along road corridors over large areas. Haala et al. (2008) and Barber et al. (2008) investigated the precision and accuracy of laser scanning point clouds collected by StreetMapper, a car-mounted MLS system, and found the technology effective for urban mapping. Kaartinen et al. (2012) studied the performance of various commercial and research-based MLS systems using a permanent test field. The results revealed that high quality point clouds can be generated under good GNSS conditions. Graham (2010) provides an overview of the most recent MLS technology. Compared to advances in MLS hardware, MLS software and automated algorithms, which are used for efficiently extracting 3D street-scene objects of interest from point clouds, are relatively slow. This is because in urban street scenes, captured point clouds contain various types of objects, such as pedestrians, cars, poles, buildings and roads. Additionally, holes often appear in the captured point clouds because of the occlusion of various objects. Although many studies have examined point cloud interpretation, such as facade and building extraction (Dold and Brenner, 2006; Rutzinger et al., 2009), pole extraction (Brenner, 2009; Lehtomäki et al., 2010), road marking extraction (Yang et al., 2012a), and point classification (Munoz et al., 2008; Yang et al., 2012b), efficient methods for the interpretation of point clouds are still in the early development stage (Yang et al., 2012b).

* Corresponding author. Tel.: +86 27 68779699; fax: +86 27 6877 8043.
E-mail address: bshyang@whu.edu.cn (B. Yang).

0924-2716/$ - see front matter © 2013 International Society for Photogrammetry and Remote Sensing, Inc. (ISPRS) Published by Elsevier B.V. All rights reserved.
http://dx.doi.org/10.1016/j.isprsjprs.2013.01.016

In this paper, we propose a high precision method for extracting 3D roads from MLS point clouds. The proposed method accurately extracts roads by utilizing global road properties (topology and smoothness) and local road features (curb borders). Related work involving road extraction from LiDAR observations is discussed in Section 2. The proposed method is described in Section 3, and classifies and recognizes road surfaces based on a geometric model of roadside curbs, which is used to detect curbs from MLS point clouds. The experimental results are listed and analyzed in Section 4, and conclusions are discussed in Section 5.

2. Literature review

Many studies have examined road extraction from airborne laser scanning (ALS) data using clustering methods that extract features based on their height differences, surface normal vector variations, and intensities (Alharthy and Bethel, 2003; Akel et al., 2005; Choi et al., 2008). Clode et al. (2007) introduce the concept of road extraction from ALS point clouds using a hierarchical classification technique, the results of which are vectorized by convolution with a complex-valued disk named the Phase Coded Disk (PCD) (Clode et al., 2004). A different technique proposed by Vosselman and Zhou (2009) elaborated on the method developed for extracting roads from ALS data when the roads are bounded by roadside curbs. Potential curb locations were detected using small height jumps near the terrain surface. This method is sensitive to the point density, which affects the completeness of the extracted lines. For the purpose of efficiently extracting road networks in large-scale urban environments, existing GIS maps are often used to estimate road locations (Hatger and Brenner, 2003; Oude Elberink and Vosselman, 2006). The given start/end points and road directions are used as initial conditions for an edge extraction algorithm that is based on deformable contour models (Göpfert et al., 2011; Boyko and Funkhouser, 2011). Map scales and generalization can negatively influence road map extraction methods. Road map registration optimizes road node positions directly from the point clouds, which is necessary for overcoming errors in the map when road extraction from raw ALS data is feasible, but the necessary level of extraction performance has not yet been achieved. In order to improve the localization accuracy and completeness of roadside detection, high-resolution digital images are used with ALS data to extract road information (Zhu et al., 2004; Hu et al., 2004). This type of automatic road extraction does not yield desirable results, because automatic image interpretation can lead to the misinterpretations of various features. In addition, image and ALS point cloud registration is still difficult.

Compared to 3D ALS point cloud scattering, MLS acquires high-density point clouds along road corridors over large areas. Road extraction from MLS point clouds is a more complicated task. Dense point clouds with high resolution and numerous street-scene objects make road segmentation and classification difficult when there is no explicit or ancillary data (e.g., intensity). Many studies have detected roads using the characteristics of horizontal plane from MLS data based on an Associative Markov Network (Munoz et al., 2008) or a region adjacency graph representation (Hernández and Matcotegui, 2009). However, searching for neighboring points in irregularly distributed point clouds is time-consuming and difficult. Therefore, some road extraction approaches fit lines to the point clouds to search for a horizontal straight line (Manandahar and Shibasaki, 2002; Yuan et al., 2008). McElhinney et al. (2010) extracted road surfaces by introducing 2D cubic spline fits to road cross sections. However, these methods often provide coarse road detections because it is hard to determine the accuracy of the road edges. Yoon and Crane (2009) used a method that determines road seeds according to the detection of road edges

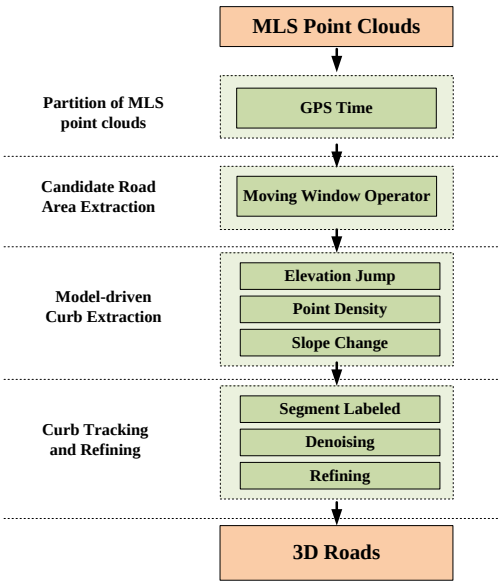

Fig. 1. Framework of extracting 3D roads from MLS point clouds.

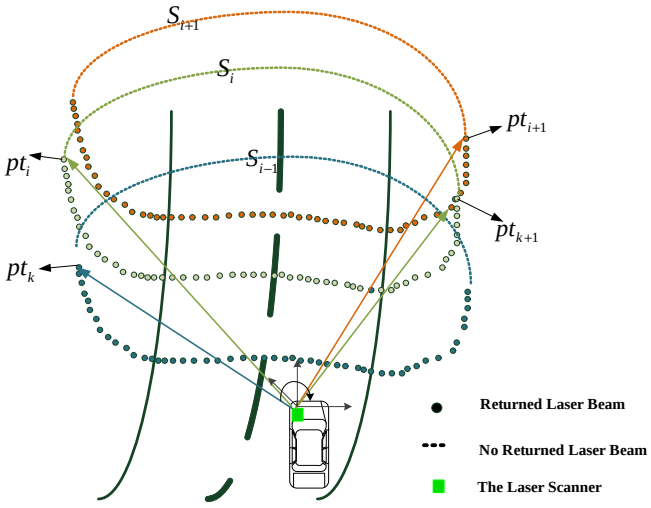

Fig. 2. Working principle of the mobile laser scanning.

(e.g., curbs) and separates each road's surface from its surrounding surface. To determine the road edges, ground lines and surfaces are further analyzed using their slope (Jaakkola et al., 2008), returned intensity, road width (McElhinney et al., 2010), and vehicle proximity (Yu and Zhang, 2006). Although these algorithms have produced promising results, previous research focuses mainly on a particular type of road (straight road) or particular scenic types (e.g., rural, urban, or highway). Prior methods may only perform well in specific conditions, and lack practical results for large-scale datasets. To analyze large-scale road environments, Zhou and Vosselman (2012) refined the curb detection method of Vosselman and Zhou (2009) with a sigmoidal function, which extracted points near the detected curbs. The road detection method has good performance for ALS point clouds. Nevertheless, it has poor performance for MLS data because parked cars can obscure curbs. Boyko and Funkhouser (2011) propose a method to extract smooth road boundaries from dense point clouds in a large-scale road environment using the ribbon snake. Road extraction from merged point clouds acquired by ALS and MLS systems take advantage of the existing 2D vector maps that indicate the candidate road

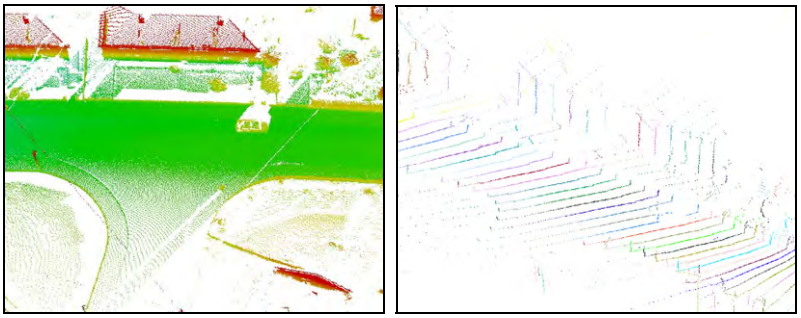

(a) MLS data (b) Segmented road sections

Fig. 3. Partitioning MLS point clouds into road cross sections.

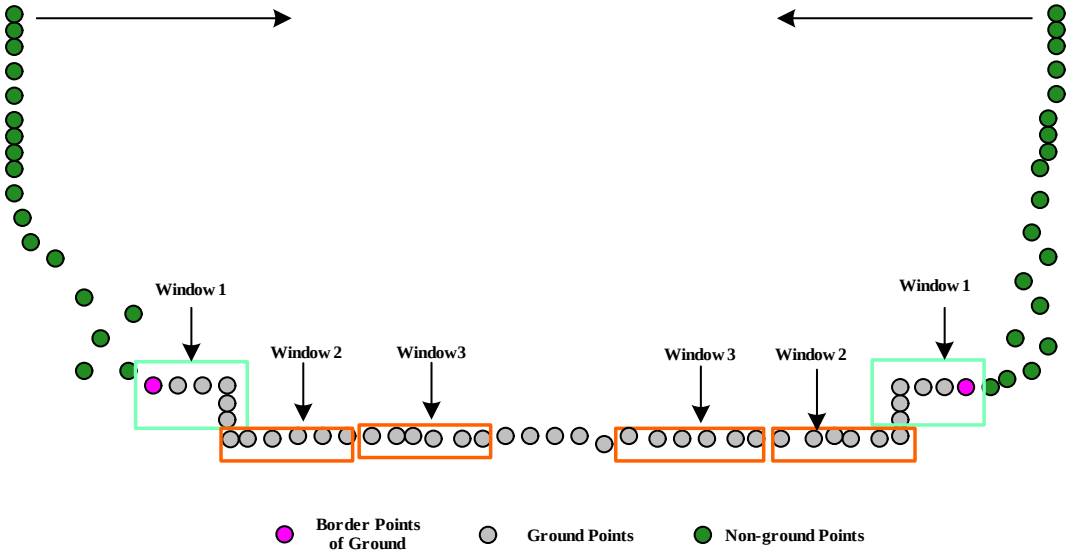

Fig. 4. Moving window filtering operator along road cross section.

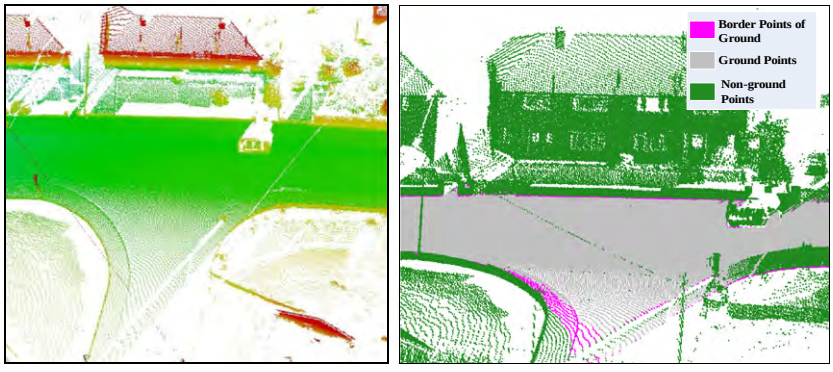

(a) raw point clouds (b) road area labeling

Fig. 5. Non-ground points filtering.

region, which involves a trade-off between efficiency and accuracy. The use of an additional information sources (e.g., GIS data) improves the modeling process, especially in terms of speed. However, this makes the model sensitive to the accuracy of the secondary database.

In this study, we present an algorithm for efficiently and accurately extracting 3D roads from MLS point clouds. In order to more cost-effectively process massive point clouds over large areas, a novel point partition technique is proposed to divide point clouds into consecutive road cross sections according to GPS time of points. Candidate road regions are sorted by cross section for further curb detection using a moving window operator. In each road cross section, curbs are detected using three popular curb patterns that account for elevation difference, point density, and slope changes. Finally, 3D road surfaces are extracted using the refined and tracked curbs. Compared with the previous methods, the

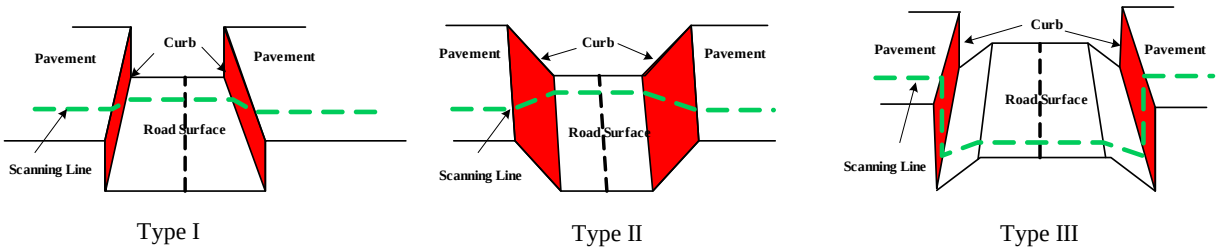

Fig. 6. Three general curb types.

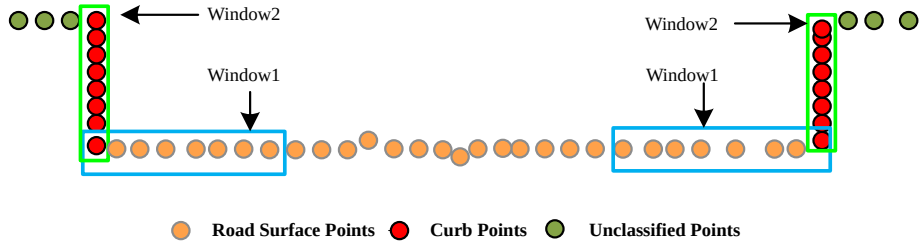

Fig. 7. Detecting curb by a moving window operator.

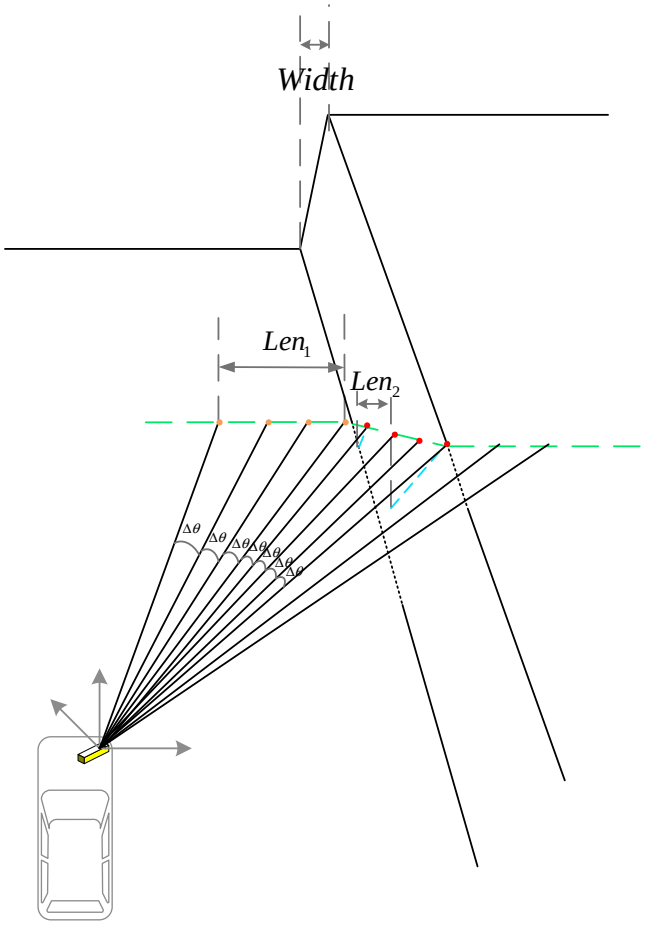

Fig. 8. Point density changes on the location of the curb according to the scanning geometry.

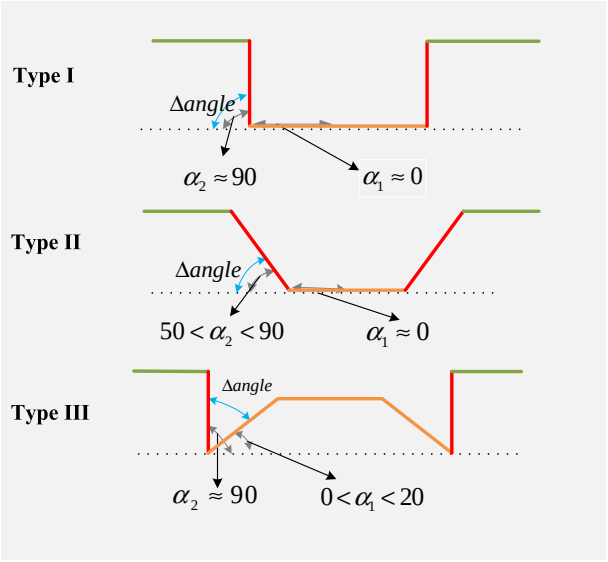

Fig. 9. The difference of the cumulative slopes in the two adjacent windows for different curb types.

proposed method can be used with large-scale point clouds without requiring a secondary dataset (e.g., images, GIS dataset), or point cloud color or intensity data. Additionally, the proposed method efficiently treats multiple types of road environments, including regular and irregular road shapes, which is critical for modeling urban environments.

3. 3D road detection

The method proposed in this paper focuses on detecting and tracking curbs from MLS point clouds as 3D road borders using both the global property of roads (e.g., topology and smoothness) and the local shape features of point clouds. The framework of the proposed method is illustrated in Fig. 1. This method encompasses four key steps:

- partitioning point clouds into road cross sections according to the GPS time of points;
- extracting candidate road areas using a moving window operator;

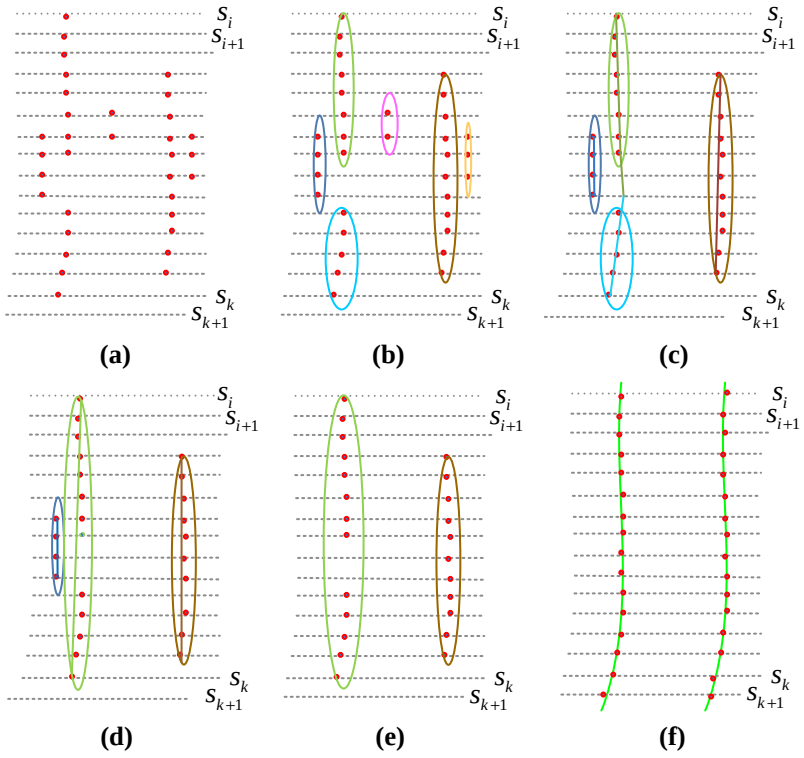

Fig. 10. Road boundaries tracing and optimization.

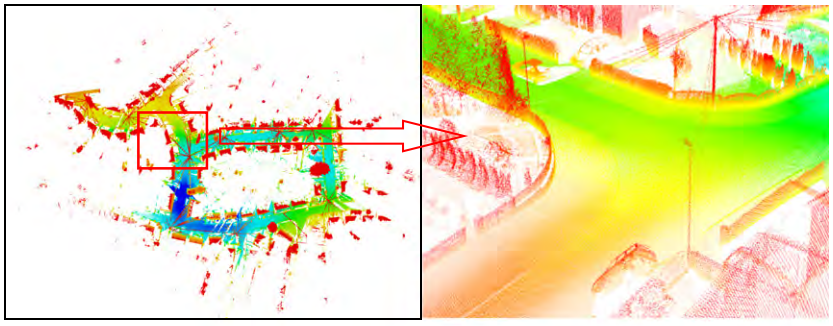

(a) Residential area

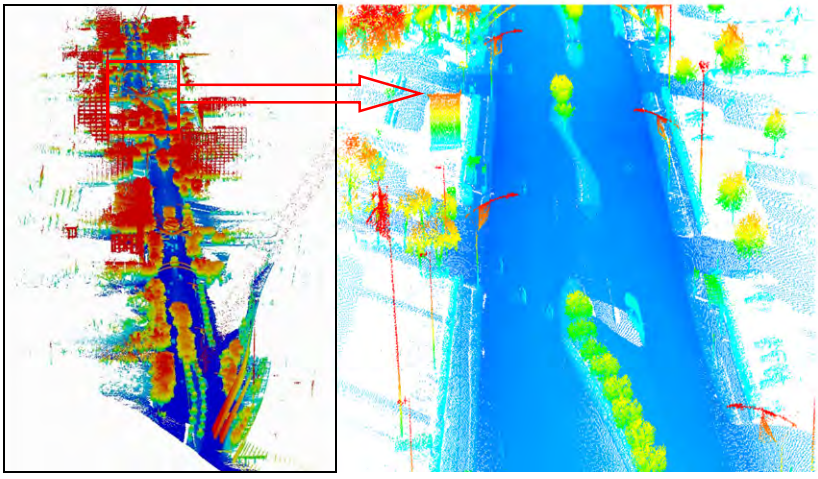

(b) Downtown area

Fig. 11. Datasets of residential and downtown area (color coded by height). (For interpretation of the references to color in this figure legend, the reader is referred to the web version of this article.)

Table 1
Road edge detection parameters used in the study.

	Description	Residential area	Downtown area
Δt	The maximum tolerance of time interval of two sequent points	$1.5 \times e^{-5}$	$1.5 \times e^{-5}$
n	The number of points in the moving window	20	20
Δh_{filter}	The maximum height of curbs	0.2 m	0.3 m
$\Delta h_{pavement}$	The maximum height difference of pavement	0.15 m	0.15 m
Δh_{curb}	The minimum height of curbs	0.1 m	0.08 m
$\Delta\theta$	The minimum slope difference between the curb and road surfaces	40 degrees	65 degrees

- detecting curb points by geometrically analyzing local points; and
- tracking and refining curbs that have both global consistency and local shape similarities.

3.1. Partition of MLS point clouds

MLS point clouds contain a huge number of points, therefore, extracting roads from point clouds is time consuming and complex. To reduce the number of points and the computational time, Boyko and Funkhouser (2011) extracted approximate road areas according to a registered vector road map, and Pu et al. (2011) fulfilled roads extraction according to vehicle trajectory data. Although the registered vector road map and vehicle trajectory data provide a feasible solution for extracting the approximate road areas from MLS point clouds, this type of secondary data may be unavailable. Additionally, tiles partitioned using these methods overlap onto areas of road intersections, resulting in difficulties for bridging road borders at neighboring patches. We aim to partition MLS point clouds into consecutive road cross sections. In light of the working principle of MLS, the laser scanner is triggered by a high precision timer and rotates at a fixed frequency. Points that are extracted from pulse echoes are sequentially recorded using a unique time marker. Assuming that all laser pulses return to the laser scanner, the time interval between two sequential laser footprints is approximately identical. However, few laser pulses will be returned from the upper view (the sky), thereby, leading to a time interval jump between the two consecutively recorded laser footprints, pt_i and pt_{i+1}, as illustrated in Fig. 2.

If the time difference between the consecutive points pt_i and pt_{i+1} is larger than the threshold value $T_{\max}$, then the two consecutive points are regarded as the breakpoints of the consecutive ith and $i+1$th road cross sections. By the breakpoints to indicate laser footprint discontinuities, the MLS point clouds can be partitioned into a set of sequential road sections using following equation:

$$pt_{i+1}(t\_gps) - pt_i(t\_gps) > T_{\max} \quad (1)$$

where $T_{\max} = 50 \times \Delta t$ and Δt is the constant time interval for sequential laser footprints.

Fig. 3 shows partition results of MLS point clouds at every twenty road cross section, according to the time intervals of laser footprints and MLS point clouds. Each color[1] in Fig. 3b indicates a separate road cross section.

Fig. 3 shows that the proposed method divides the MLS point clouds into a set of sequential road cross sections. The partition method has several advantages: (1) it is easy to segment MLS point clouds without the support of secondary data (e.g., trajectory data); (2) each segmented road cross section maintains road properties such as curb points; and (3) each segmented road cross section has a small number of points and is easily dealt with for further road extraction.

[1] For interpretation of color in Figs. 3,6 and 16, the reader is referred to the web version of this article.

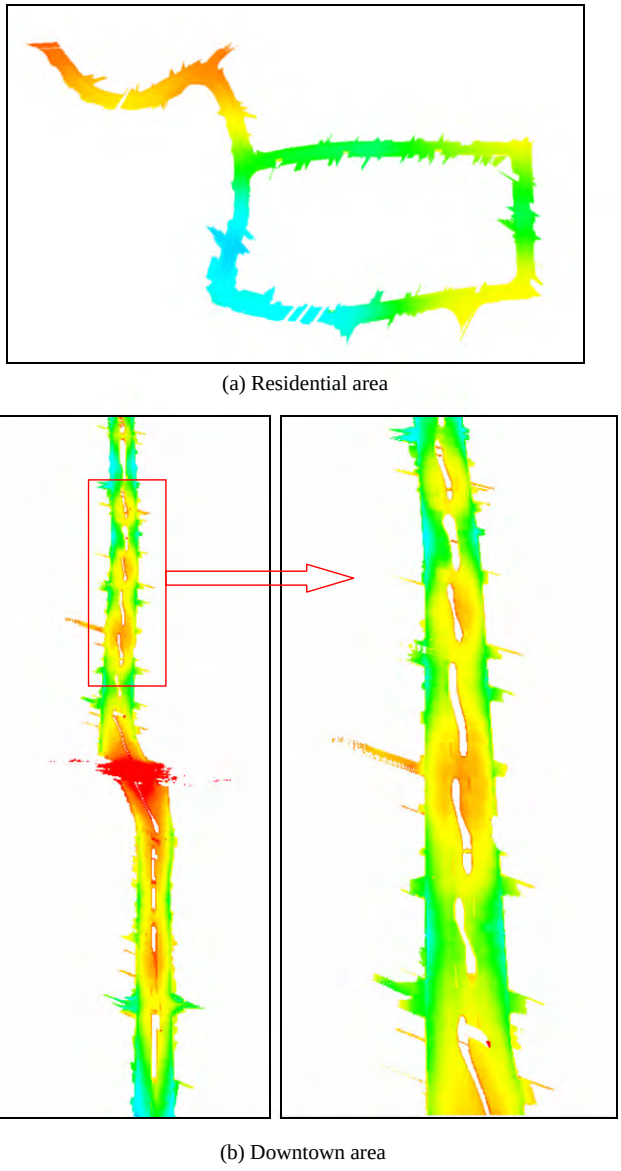

(a) Residential area

(b) Downtown area

Fig. 12. The candidate road area extraction (color coded by height). (For interpretation of the references to color in this figure legend, the reader is referred to the web version of this article.)

3.2. Extraction of candidate road areas

The MLS point clouds are partitioned into road cross sections according to the procedure described in Section 3.1. Each road cross section can have points from buildings, cars, pedestrians, and poles. Typically, objects at different distances from a sensor can be in a single scan line. Fig. 3b shows the differences between the point distributions of buildings and roads. To extract the candidate road area from the cross section, non-ground points

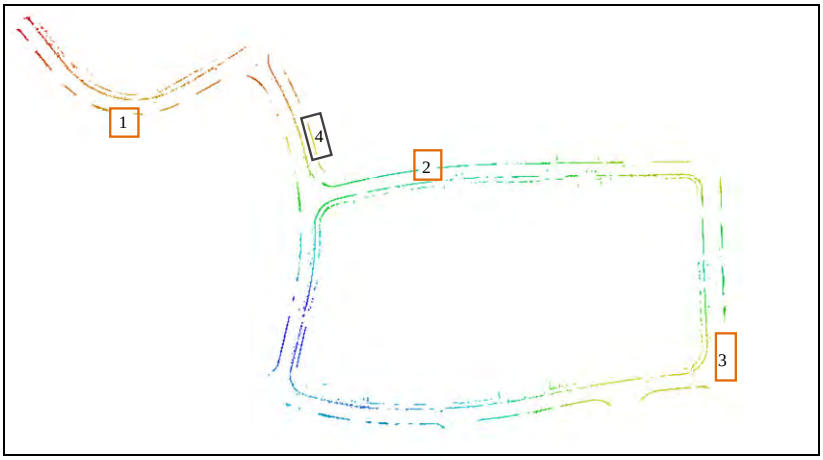

(a) The detected curb point in residential data (1, 2, and 3 indicating gaps by occlusion, 4 indicating faked curb points).

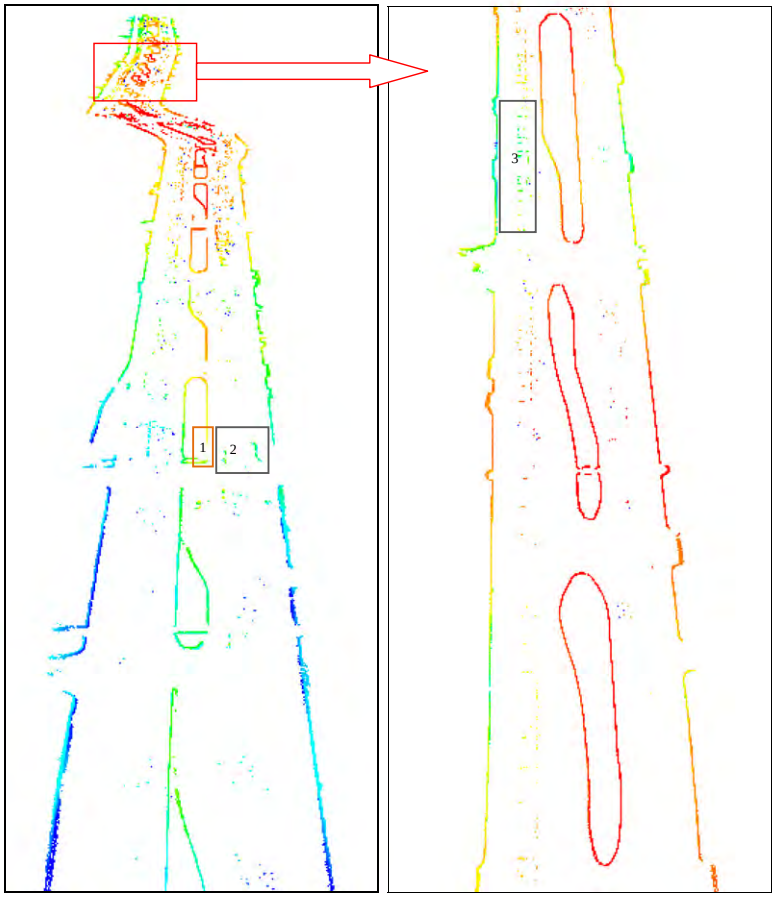

(b) The detected curb points in downtown data (1 indicating gap by occlusion, 2 and 3 indicating fake curb points)

Fig. 13. The results of curb extraction (color coded by height). (For interpretation of the references to color in this figure legend, the reader is referred to the web version of this article.)

should be filtered out. In general, road points at one cross section have an almost identical elevation to points on the road, and non-ground points have a higher elevation than points on the road. Therefore, the filtering of non-ground points was conducted using 1-D line filtering based on elevation differences between the road and the ground. To completely filter out non-ground points, we implemented a moving window operator that searched for elevation jumps for points along road cross sections. The moving window filtering operator has three adjacent windows that slide along each road cross section from the outer edge to the middle edge, as illustrated in Fig. 4. The filtering operators in the three adjacent windows are as follows:

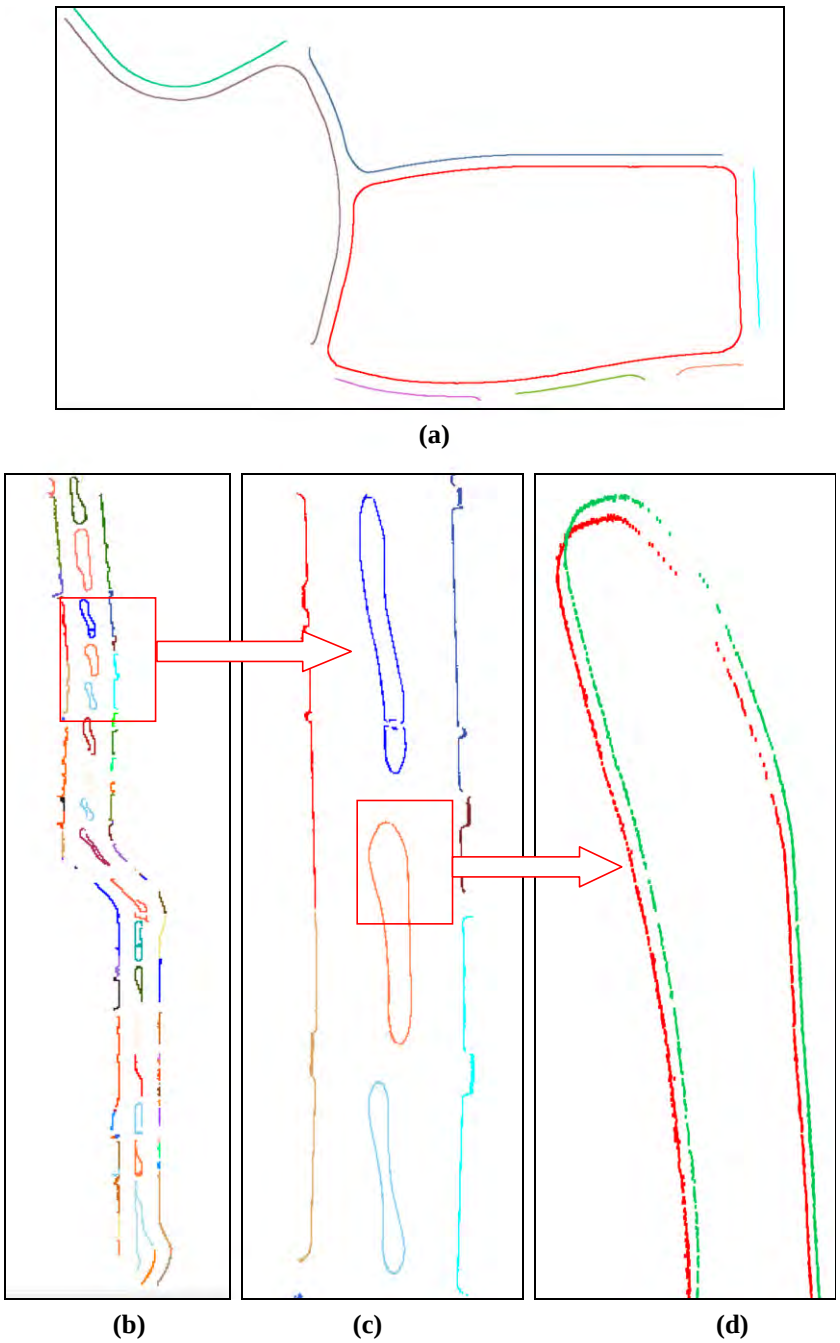

Fig. 14. Results of curb tracking and refining: (a) residential area; (b) downtown area; (c) enlarged for detailed inspection of the results of downtown area; (d) the top and bottom of the curb points plotted by red and green (the green strip is the borders of road surfaces). (For interpretation of the references to color in this figure legend, the reader is referred to the web version of this article.)

$$\Delta h_{pavement} \leqslant \Delta Z_1 \leqslant \Delta h_{fiter} \tag{2}$$

$$\Delta Z_2 \leqslant \Delta h_{pavement} \tag{3}$$

$$\Delta Z_3 \leqslant \Delta h_{pavement} \tag{4}$$

where $\Delta Z_i = \max(Z_i) - \min(Z_i)(i = 1{:}3)$ is the maximum elevation difference in each window, $\Delta h_{pavement}$ is the threshold of the maximum elevation difference of pavement, and Δh_{filter} is the relative elevation of pavement to the ground. $\Delta h_{pavement}$ implying that the points in window$_2$ and window$_3$ fit a horizontal line segment. The length of each window is determined by the number of points (n) located in the window. Empirically, n is more than 20.

Results after filtering with the moving window operator are illustrated in Fig. 5. Fig. 5a shows the original point clouds. In Fig. 5b, the candidate road points are plotted in gray with border points distinctly plotted in magenta. Non-ground points are plotted in forest green. It appears that the non-ground points (e.g., buildings, trees, and cars) are labeled well and the ground points are well preserved.

3.3. Model-driven curb extraction

In order to extract roads from the set of ground points, it is necessary to detect the curb points that separate the pavement

Fig. 15. Road extraction and details from the residential data.

and roads. A curb is as adjacent region between roads and pavement/green belts. Curbs are regarded as road boundaries. In general, curbs have three main types, which are illustrated in Fig. 6. Fig. 6 shows that there is an elevation and slope jump at the curb (the red dotted location). After curb detection, road borders can be identified. Type I curbs border flat roads which have only a small elevation jump between the road and curb surfaces. Type II curbs display a gradual height change between the road and curb surfaces. Type III curbs occur between pavement and roads where the road has a curvature near the road border.

To find the curb location, we analyzed the characteristics of points at each road cross section using three indicators: elevation jump, point density, and slope change. From the middle to the outer edge of each road cross section, two adjacent moving windows of a specified length were designed to slide point by point along the candidate road cross section, as illustrated in Fig. 7. The number of points in each window is identical. We calculated the elevation jump, point density, and slope change in each window. Curb points were detected by defining a set of rules for elevation jump, point density, and slope change for a set of points to be classified as a curb and according to curb types.

3.3.1. Rule-1: elevation jump

If one of the two windows covers a curb, the elevation jump in the two windows should meet the following constraint conditions:

$$\Delta Z_{curb\_1} \leqslant \Delta h_{pavement} \tag{5}$$

$$\Delta Z_{curb\_2} \geqslant \Delta h_{curb} \tag{6}$$

where $\Delta Z_{curb\_i} = \max(Z_i) - \min(Z_i)(i = 1{:}2)$ is the maximum elevation difference in window$_1$ or window$_2$.

The above constraint specifies that the elevation jump in the first window is less than a height of $\Delta h_{pavement}$, implying that the points in the first window are road points. The elevation jump in the second window is more than the minimum height of the curb, Δh_{curb}, implying that the points in the second window belong to a curb.

3.3.2. Rule-2: point density

Because of the laser scanning principle, the point span depends on the distance and incidence angle between the object and the scanner. Surfaces that are nearly parallel to the laser pulses have a rather low point density. However, surfaces that are perpendicular to the laser pulses have a much higher point density (Lehtomäki et al., 2010). Therefore, more points are located on curbs than on neighboring roads (Fig. 8). This implies that the span between sequential points on the road along a cross section is longer than that on the curb. The length of each window is described by the Euclidean distance calculated by $Len = \sqrt{(x_1 - x_{n_1})^2 + (y_1 - y_{n_1})^2}$. If one of the two windows covers a curb location, then the length of window$_1$ and window$_2$ must satisfy the following condition:

$$Len_2 < L < Len_1 \tag{7}$$

In most road environments, typically, the width of the curb is relatively narrow, so we set the value of L at 0.3 m.

3.3.3. Rule-3: slope change

Bearing in mind the three curb types, there will be a significant slope change if one of the two windows covers a curb. Therefore, the slope between any two adjacent points in each window is calculated and summed as a cumulative slope α to detect the curb. The cumulative slope α in each window is calculated by

$$\alpha = \sum_{i=1}^{n_1} \arctan\left[\frac{(z_i - z_{i+1})}{\sqrt{(x_i - x_{i+1})^2 + (y_i - y_{i+1})^2}}\right] \tag{8}$$

where (x,y,z) is the coordinate of point in each window, and n_1 is the size of the window, which is defined by $n_1 = n/2$.

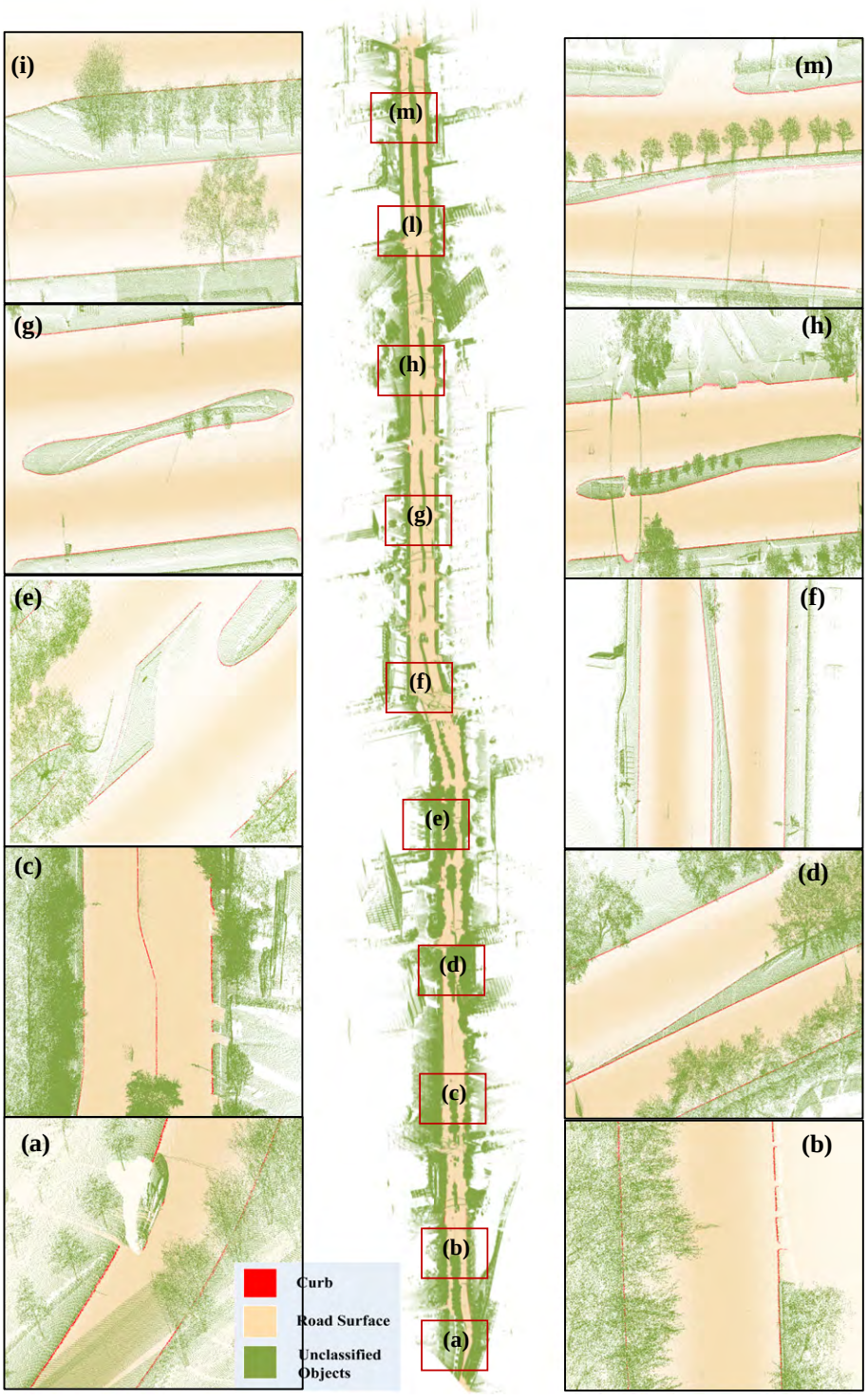

Fig. 16. Road extraction and details from the downtown data.

The cumulative slope of each type of curb is shown in Fig. 9. For each curb type, there will be an abrupt angle between the road and the curb surfaces. Therefore, the difference between the cumulative slopes of the two adjacent windows is calculated using Eq. (9), and represents the angle between the road and curb surfaces.

$$\Delta angle = abs(\alpha_1 - \alpha_2) \tag{9}$$

$$\Delta angle = \Delta\theta \tag{10}$$

where $\Delta\theta$ is the minimum angle tolerance between the road and curb surfaces.

Using the above three indicators, the points for window$_2$ are defined as the points located on the curb from each partitioned road section. The upper and lower points of the curb surface are also identified. The lower points of the curb surface are considered as the border points of the road that will be traced and refined.

3.4. Tracing and refining curb for road delineation

In street scenes, the detected curb points are discontinuous because curbs are sometimes absent or blocked by cars. In addition,

Fig. 17. Registration of extracted curb points and the Google Earth image (residential area).

obstacles such as low barriers have geometric patterns similar to curbs' and therefore might be confused with curbs and introduce fake curb points. Because the detected curb is only a set of points and does not contain topology, it is necessary to track and refine curb points to delineate road boundaries.

The proposed method uses the locally similar geometric patterns of curb points at sequential road cross sections to trace and refine the curb points. The main steps are as follows:

(a) *Segment labeling*: The k-nearest neighbor (k-NN) method classifies the curb points into segments. The Euclidean distances and angles between the curb points are calculated and used as distance metrics. In a local area, the curb points are distributed along approximately straight lines (Fig. 10a). Fig. 10b illustrates segments labeled using the k-NN method.
(b) *Noise removal*: To eliminate the fake segments that contain few points, the segments of less than three points are eliminated, as illustrated in Fig. 10c.
(c) *Refinement*: The remaining segments will be connected if two adjacent segments are approximately collinear (Fig. 10d). The connected segments are sorted along the direction of the segments. Outer segments with small lengths are discarded. Fig. 10e shows a result for curb points processed using this method.

For regular roads, the refined curb points that constitute the initial roadside are extended line by line to close the gap or to add the edge points with the property of parallel lines. Additionally, a B-spline algorithm is used to generate smooth curves (Fig. 10f).

4. Results and analysis

4.1. Test data

The test data sets were acquired using the Optech's Lynx Mobile Mapper System. The Lynx is equipped with two laser scanners, which are mounted perpendicular to each other. The two laser scanners are oriented at an angle of 45° from the driving direction, and collect data at a rate of 500,000 measurements per second with a field of view (FOV) of 360 degrees. The data shown in Fig. 11a is a residential area, which has a typical urban road with structured road boundaries in the form of curbs. The scene contains many low fences and cars that are geometrically similar to curbs. The data set covers an area of 460 m * 375 m with roughly 8 million points. The data set from the downtown area shown in Fig. 11b is a complex street scene with multiple lanes and irregular road boundaries that are approximately 2.2 km in length and have 32 million points. Furthermore, the street scene contains numerous grass strips, trees, poles, and electric wires, which contribute the complexity of road extraction and delineation.

4.2. 3D Road extraction results

Based on the proposed method, the time interval threshold of two sequential points was specified as $1.5 \times e^{-5}$ according to the parameters of the Lynx system for partitioning the MLS point clouds into road cross sections. Then, the values of Δh_{filter}, $\Delta h_{pavement}$, and Δh_{curb} were also specified for filtering out non-ground points and extracting the curb points. The values of the parameters

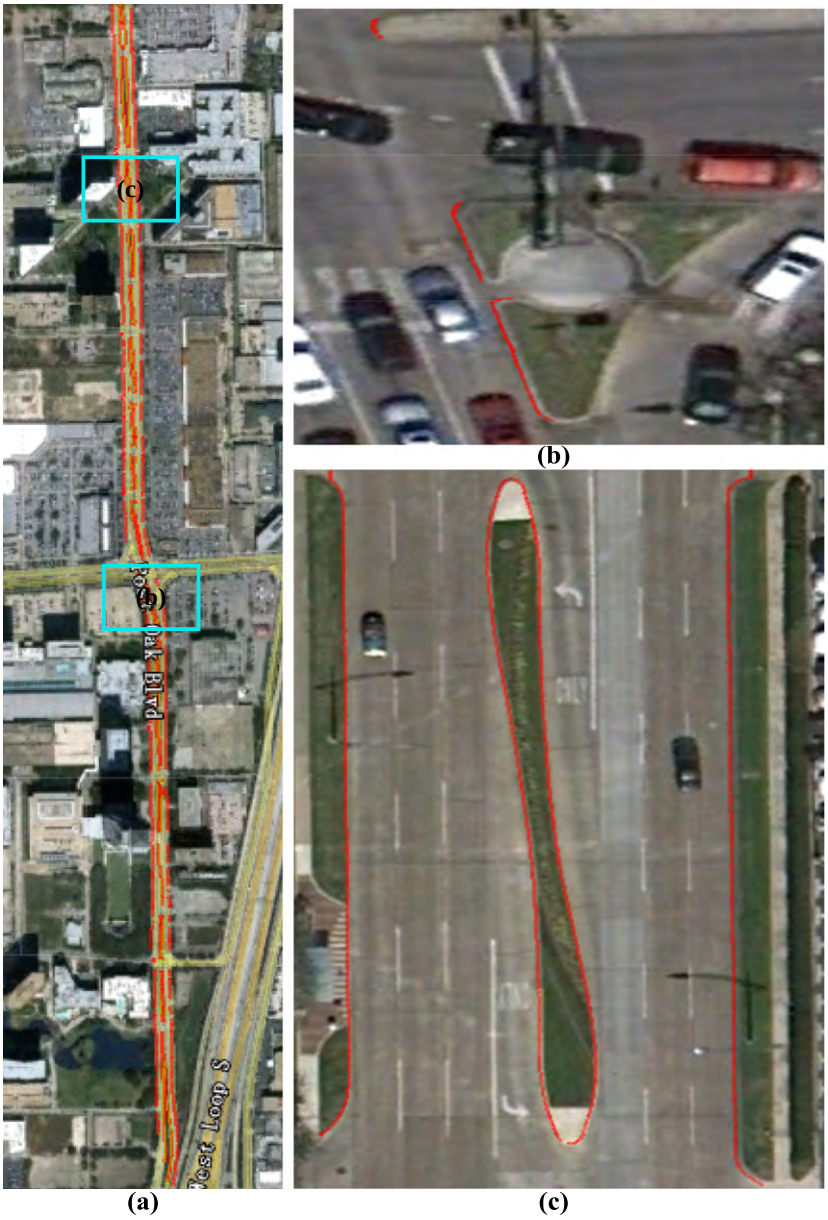

Fig. 18. Registration of extracted curb points and the Google Earth image (downtown area).

for the study are listed in Table 1. Typically, the curb height is about 0.15 m. In order to detect the grass strip and raised median borders, the maximum and minimum curb height thresholds are set to 0.2 m and 0.1 m for the residential area, and 0.3 m and 0.08 m for the downtown area. The minimum tolerance angle between road and curb surfaces, $\Delta\theta$, was set to 40 degrees and 65 degrees for the residential and downtown areas, respectively.

Fig. 12 shows the results of candidate road area extraction for the residential and downtown areas. The candidate road areas show a fairly flat distribution, which indicates that the filtering operator is effective at detecting candidate road areas from MLS point clouds. The detected candidate road areas were used to detect curb points using the model-driven curb extractor. Fig. 13 shows that the curb extraction results for the residential and downtown areas are satisfactory. However, many points on the bottom of cars and fences were falsely identified as curb points. Additionally, several gaps appear in the detected curb lines because of road intersections or vehicle obstructions. Finally, the detected curb points were tracked and refined to eliminate the fake points and to bridge the gaps. Fig. 14 illustrates curbs plotted with different colors. Each color denotes a different 3D road border. As in the residential area, roads have regular shapes and a fixed width. The 3D road borders were interpolated using B-splines which connected several of the gaps. However, because the roads in the downtown area have irregular shapes, the gaps were difficult to close.

In order to check the quality of 3D road extraction, the boundaries of the extracted roads were overlaid with the MLS point clouds for visual checking, as illustrated in Figs. 15 and 16. Different parts of the test data sets have been enlarged for detailed inspection. Our analysis indicates that the proposed method effectively detects curb points, even in the locations where roads have curved shapes, as illustrated in Fig. 15b. In addition, the proposed method extracts the borders of green belts and raised medians, as shown in Fig. 16b–e. A visual check shows that the proposed method performs well in most cases but may fail to extract curb

points for locations where the density of points is low (as illustrated in Fig. 15e). These locations are far away from the laser scanner and have few points, which cause difficulties in the curb extraction process. However, there are still only a few fake curb points (Fig. 16a), and these points show very similar patterns to curb points and are close to the road boundary.

4.3. Quantitative evaluation of 3D road extraction

For a visual check the relative accuracy of the extracted 3D roads, the detected road boundaries were transformed into the Keyhole Markup Language (KML) format and superimposed with Google Earth images. Figs. 17 and 18 show the results of overlapping the road boundaries with Google Earth images. The extracted road boundaries match the border of the roads on Google Earth images, even at traffic island locations, as shown in Fig. 18b.

To evaluate the completeness of the road extraction, we firstly manually extracted roads from the test datasets by digitizing the road borders from the ortho-images of the test areas as the reference or ground truth data, and then compared the reference road borders with those extracted by the proposed method. We calculated the following three accuracy metrics, which are widely used for the evaluation of road extraction algorithms (e.g., Heipke et al., 1997; Clode et al., 2007):

- *Completeness* = TP/L_r
- *Correctness* = TP/L_e
- *Quality* = $TP/L_e + FN$

where L_r is the total length of the reference road, L_e is the total length of the extracted road, $TP = \min(L_{me}, L_{mr})$, L_{me} is the total length of the extracted road that matches the reference road, and L_{mr} is the total length of the reference road that matches the extracted road.

The values of the *FN* and *FP* of the two datasets listed in Table 2 were calculated based on the manually extracted roads. The value of *FN* is the total length of the reference road unmatching with the extracted road. In contrast, FP is the total length of the extracted road unmatching with the reference road. The lengths of the curbs (LCs) extracted with the proposed method from the two datasets were calculated to compare with manually extracted results.

Table 2
The *FNs* and *FPs* of reference data.

	FN (m)	*FP* (m)
Residential area	85.25	32.36
Downtown area	410.26	335.73

Table 3
The lengths of the extracted curb: *LCs and TPs*.

	LC (m)	*TP* (m)
Residential area	1697.70	1665.34
Downtown area	8350.50	8014.77

Table 4
The accuracy of the curb extraction results.

	Completeness (%)	Correctness (%)	Quality (%)
Residential area	95.13	98.09	93.40
Downtown area	95.13	95.98	91.48

Table 3 lists the LCs and TPs of the extracted curbs. The TPs of the extracted curbs represent the difference between the LCs and FPs. Table 4 lists the correctness, the completeness, and the quality of the proposed method for the two datasets.

Table 4 shows that for the two datasets, the proposed method achieves an accuracy of over 95%, completeness of over 94%, and a quality of 91%. The intersections of detection roads are a major contribution to the *FN* in the residential area. There are still some *FP* detections at car bottoms. Though uncommon in the residential area, in the downtown area the gaps caused by moving cars are a major contribution to the *FN*. Additionally, a major contribution to the *FP* is found to be the entrances to the pavement, which result in a slight drop of completeness in the downtown area. Based on these results, the proposed method appears to work reliably for various street scenes.

5. Conclusion

Efficient methods for extracting roads from the dense and huge volume point clouds collected by MLS systems are of vital importance. We have proposed a novel method for the extraction and delineation of 3D roads from MLS point clouds. The proposed method utilizes the working principle of the MLS system and the GPS time of the point clouds to successfully separate the point clouds of the MLS system into a set of sequential road cross sections. A window based filtering operator was implemented to filter non-ground points from each road cross section. Three general types of curbs are modeled and integrated in the proposed method, which detects the curb points from filtered point clouds using a set of defined rules for elevation jump, point density, and slope change. The proposed method successfully extracts and delineates 3D roads by tracking and refining the detected curb points. Experiments validated the use of the proposed method for two different test areas. Visual inspection and quantitative evaluation showed that the proposed method is effective at extracting 3D roads from MLS point clouds, even in complex urban street-scenes.

Although the proposed method extracts 3D roads from the tested datasets with good completion, correctness, and quality, the values of the parameters are critical for the performance of the proposed method. Particularly, the length of the moving window for filtering non-ground points has an effect on the detection of road areas. Suppose that the length of the window is less than the width of curbs. The points near the curb may falsely be labeled as curb points. Meanwhile, the variations of local and global point densities make it difficult to select the moving window length. However, the proposed method was only tested using different urban scenes, where the road curb boundaries had elevation jumps and slope changes. It is also difficult for the proposed method to deal with curbs with boundaries that are characterized as asphalt/soil, asphalt/vegetation, or asphalt/grassy bank. In the near future, the intensity of the point clouds or the registered imagery can be incorporated in the proposed method to detect the boundary of such kind of curbs, and the practical usefulness of the proposed method will be tested with the point clouds collected by other commercial and research-based MLS systems.

Acknowledgments

Work described in this paper was jointly supported by National Basic Research Program of China (No. 2012CB725301), the NSFC project (No. 41071268), and the Fundamental Research Funds for the Central Universities (No. 3103005). Special thanks go to Editor and anonymous reviewers for their constructive comments that substantially improve quality of the paper.

References

Akel, N.A., Kremeike, K., Filin, S., Sester, M., Doytsher, Y., 2005. Dense DTM generalization aided by roads extracted from LIDAR data. International Archives of the Photogrammetry, Remote Sensing and Spatial Information Science 36 (Part 3/W19), 54–59.

Alharthy, A., Bethel, J., 2003. Automated road extraction from Lidar data. In: Proc. ASPRS Annual Conference, Anchorage, Alaska, unpaginated CD-Rom.

Barber, D., Mills, J., Smith, V.S., 2008. Geometric validation of a ground-based mobile laser scanning system. ISPRS Journal of Photogrammetry and Remote Sensing 63 (1), 128–141.

Barsi, A., Heipke, C., 2003. Artificial neural networks for the detection of road junctions in aerial images. International Archives of Photogrammetry, Remote Sensing and Spatial, Information Sciences 34 (Part3/W8), 17–19.

Boyko, A., Funkhouser, T., 2011. Extracting roads from dense point clouds in large scale urban environment. ISPRS Journal of Photogrammetry and Remote Sensing 66 (6), S2–S12.

Brazohar, M., Cooper, D.B., 1996. Automatic finding of main roads in aerial images by using geometric-stochastic models and estimation. IEEE Transactions on Pattern Analysis and Machine Intelligence 18 (7), 707–721.

Brenner, C., 2009. Extraction of features from mobile laser scanning data for future driver assistance systems. Advances in GIScience, Lecture Notes in Geoinformation and Cartography. Springer, pp. 25–42.

Clode, S., Rottensteiner, F., Kootsookos, P., Zelniker, E., 2007. Detection and vectorization of roads from Lidar data. Photogrammetric Engineering & Remote Sensing 73 (5), 517–536.

Clode, S., Zelniker, E., Kootsookos, P., Clarkson, V., 2004. A phase coded disk approach to thick curvilinear line detection. In: Proceeding of 17th European Signal Processing Conference, EUSIPCO, pp. 1147–1150.

Choi, Y.W., Jang, Y.W., Lee, H.J., Cho, G.S., 2008. Three- dimensional LiDAR data classifying to extract road point in urban area. IEEE Geoscience and Remote Sensing Letters 5 (4), 725–729.

Dold, C., Brenner, C., 2006. Registration of terrestrial laser scanning data using planar patches and image data. International Archives of Photogrammetry, Remote Sensing and Spatial Information Sciences 36 (Part 5), 25–27.

Ferchichi, S., Wang, S., 2005. Optimization of cluster coverage for road centre-line extraction in high resolution satellite image. In: International Conference on Image Processing, pp. 201–204.

Göpfert, J., Rottensteiner, F., Heipke, C., 2011. Using snake for the registration of topographic road database objects to ALS features. ISPRS Journal of Photogrammetry and Remote Sensing 66 (6), 858–871.

Graham, L., 2010. Mobile mapping system overview. Photogrammetric Engineering & Remote Sensing 76 (3), 222–229.

Haala, N., Peter, M., Cefalu, A., Kremer, J., 2008. Mobile lidar mapping for urban data capture. In: Proceedings of the 14th International Conference on Virtual Systems and Multimedia, Limassol, Cyprus, 20–25 October, pp. 95–100.

Hatger, C., Brenner, C., 2003. Extraction of road geometry parameters from laser scanning and existing database. International Archives of Photogrammetry, Remote Sensing and Spatial Information Sciences 34 (Part 3/W13), 225–230.

Heipke, C., Mayer, H., Wiedeman, C., Jamet, O., 1997. Evaluation of automatic road extraction. International Archives of Photogrammetry, Remote Sensing and Spatial Information Sciences 32 (Part 3/W3), 47–56.

Hernández, J., Matcotegui, B., 2009. Filtering of artifacts and pavement segmentation from mobile Lidar data. International Archives of the Photogrammetry, Remote Sensing and Spatial Information Sciences 38 (Part 3/W8), 329–333.

Hu, X., Tao, C.V., Hu, Y., 2004. Automatic road extraction from dense urban area by integrated processing of high-resolution imagery and LIDAR data. International Archives of Photogrammetry, Remote Sensing and Spatial Information Sciences 35 (Part B3), 288–292.

Jaakkola, A., Hyyppä, J., Hyyppä, H., Kukko, A., 2008. Retrieval algorithms for road surface modelling using Laser-based mobile mapping. Sensors 8 (9), 5238–5249.

Kaartinen, H., Hyyppä, J., Kukko, A., Jaakkola, A., Hyyppä, H., 2012. Benchmarking the performance of Mobile Laser Scanning Systems using a permanent test field. Sensors 12 (9), 12814–12835.

Lacoste, C., Descombes, X., Zerubia, J., 2005. Point process for unsupervised line network extraction in remote sensing. IEEE Transaction on Pattern Analysis and Machine Intelligence 27 (10), 1568–1579.

Lacoste, C., Descombes, X., Zerubia, J., 2010. Unsupervised line network extraction in remote sensing using a polyline process. Pattern Recognition 43, 1631–1641.

Lafarge, F., Gimelfarb, G., Descombes, X., 2010. Geometric feature extraction by a multi-marked point process. IEEE Transaction on Pattern Analysis and Machine Intelligence 32 (9), 1597–1609.

Laptev, I., Mayer, H., Lindeberg, T., Eckstein, W., Steger, C., Baumgartner, A., 2000. Automatic extraction of roads from aerial images based on scale space and snakes. Machine Vision and Applications 12 (1), 23–31.

Lehtomäki, M., Jaakkola, A., Hyyppä, J., Kukko, A., Kaartinen, H., 2010. Detection of vertical pole-like objects in a road environment using vehicle-based laser scanning data. Remote Sensing 2 (3), 641–664.

Manandahar, D., Shibasaki, R., 2002. Auto-extraction of urban features from vehicle-borne laser data. International Archives of Photogrammetry, Remote Sensing and Spatial, Information Sciences 34 (Part4), 433–438.

McElhinney, C., Kumar, P., Cahalane, C., McCarthy, T., 2010. Initial results from European road safety inspection (EURSI) mobile mapping project. International Archives of Photogrammetry, Remote Sensing and Spatial Information Sciences 38 (Part 5), 440–445.

Munoz, D., Vandapel, N., Hebert, M., 2008. Directional associative markov network for 3-d point cloud classification. In: Proc. 4th International Symposium on 3D. Data Process, Visualization and Transmission, Atlanta, GA, 18–20 Jun, pp. 1–8.

Niu, X., 2006. A semi-automatic framework for highway extraction and vehicle detection based on a geometric deformable model. ISPRS Journal of Photogrammetry and Remote Sensing 61 (3–4), 170–186.

Oude Elberink, S., Vosselman, G., 2006. Adding the third dimension to a topographic database using airborne laser scanner data. International Archives of Photogrammetry, Remote Sensing and Spatial Information Sciences 36 (Part 3), 92–97.

Peng, T., Jermyn, I.H., Prinet, V., Zerubia, J., 2008. An extended phase field higher-order active contour model for networks and its application to road network extraction from vhr satellite image. In: Proceedings of 10th European Conference on Computer Vision, Springer-Verlag, Heidelberg, pp. 509–520.

Pu, S., Rutzinger, M., Vosselman, G., Oude Elberink, S., 2011. Recognizing basic structures from mobile laser scanning data for road inventory studies. ISPRS Journal of Photogrammetry and Remote Sensing 66 (6), S28–S39.

Rutzinger, M., Oude Elberink, S., Pu, S., Vosselman, G., 2009. Automatic extraction of vertical wall from mobile and airborne laser scanning data. International Archives of Photogrammetry, Remote Sensing and Spatial Information Science 38 (Part 3/W8), 74–79.

Vosselman, G., Zhou, L., 2009. Detection of curbstones in airborne laser scanning data. International Archives of Photogrammetry, Remote Sensing and Spatial Information Science 37 (Part 3/W8), 111–116.

Wan, Y., Shen, S., Song, Y., Liu, S., 2007. A road extraction approach based on fuzzy logic for high-resolution multispectral data. In: Fourth International Conference on Fuzzy Systems and Knowledge Discovery, IEEE Computer Society, Los Alamitos, CA, USA, pp. 203–207.

Yang, B.S., Fang, L.N., Li, Q.Q., Li, J., 2012a. Automated extraction of road markings from mobile lidar point clouds. Photogrammetric Engineering & Remote Sensing 78 (4), 331–338.

Yang, B.S., Wei, Z., Li, Q.Q., Li, J., 2012b. Automated extraction of street-scene objects from mobile lidar point clouds. International Journal of Remote Sensing 33 (18), 5839–5861.

Yoon, J., Crane, C.D., 2009. Evaluation of terrain using LADAR data in urban environment for autonomous vehicles and its application in the DARPA urban challenge. In: ICCAS-SICE International Joint Conference 2009, IEEE, Fukuoka, Japan, 18–21 August, pp. 641–646.

Yuan, X., Zhao, C.X., Cai, Y.F., Zhang, H.F., 2008. Road-surface abstraction using lidar sensing. In: 2008 10th Intel. Conf. on Control, Automation, Robotics and Vision Hanoi, Vietnam, 17–20 December, pp. 1097–1102.

Yu, C., Zhang, D., 2006. Road curbs detection based on laser radar. In: 8th International Conference on Signal Processing, IEEE, Beijing, China, 16–20 November, pp. 8–11.

Zhang, C., Baltsavias, E., Gruen, A., 2001. Knowledge-based image analysis for 3D road construction. Asian Journal of Geoinformatica 1 (4), 3–14.

Zhou, L., Vosselman, G., 2012. Mapping curbstones in airborne and mobile laser scanning data. International Journal of Applied Earth Observation and Geoinformation 18 (2012), 293–304.

Zhu, P., Lu, Z., Chen, X., Honda, K., Eiumnoh, A., 2004. Extraction of city roads through shadow path reconstruction using laser scanning. Photogrammetric Engineering & Remote Sensing 70 (12), 1433–1440.